Separation Science and Technology
Publication details, including instructions for authors and subscription information:
http://www.informaworld.com/smpp/title~content=t713708471

Study of Polarization Phenomena in Membrane Distillation of Aqueous Salt Solutions

L. Martínez-Díez[a]; F. J. Florido-Díaz[a]; M. I. Vázquez-González[a]
[a] DEPARTAMENTO DE FÍSICA APLICADA, UNIVERSIDAD DE MÁLAGA, MÁLAGA, SPAIN

To cite this Article Martínez-Díez, L. , Florido-Díaz, F. J. and Vázquez-González, M. I.(2000) 'Study of Polarization Phenomena in Membrane Distillation of Aqueous Salt Solutions', Separation Science and Technology, 35: 10, 1485 — 1501

To link to this Article: DOI: 10.1081/SS-100100237

URL: http://dx.doi.org/10.1081/SS-100100237

SEPARATION SCIENCE AND TECHNOLOGY, **35**(10), pp. 1485–1501, 2000

Study of Polarization Phenomena in Membrane Distillation of Aqueous Salt Solutions

L. MARTÍNEZ-DÍEZ,* F. J. FLORIDO-DÍAZ, and
M. I. VÁZQUEZ-GONZÁLEZ
DEPARTAMENTO DE FÍSICA APLICADA
FACULTAD DE CIENCIAS
UNIVERSIDAD DE MÁLAGA
29071 MÁLAGA, SPAIN

ABSTRACT

In this paper we study water transport in membrane distillation using a flat PTFE membrane. Experiments have been carried out with water and aqueous solutions of NaCl as feed. The effects of temperature and concentration polarization on the reduction of vapor pressure differences across the membrane with regard to the vapor pressure differences corresponding to the bulk phases which are separated by the membrane have been evaluated. A coefficient which measures this reduction has been introduced. This coefficient and the known temperature polarization coefficient coincide when water is used as feed, but they are more and more different when the salt concentration of feed increases. In this last case it is the polarization coefficient introduced here that measures the reduction of flux through the effect of the polarization phenomena. The measured flux results and the calculated polarization results are discussed for different temperatures, recirculation rates, and feed concentrations.

INTRODUCTION

Membrane distillation (MD) is a transport process using hydrophobic microporous membranes. In the MD process studied here, we have a salt aqueous solution at an elevated temperature on one side of the membrane and pure water on the other side. Neither media penetrates the microporous membrane, and a liquid–vapor interface is formed on each side of the membrane. The tem-

---

* To whom correspondence should be addressed. E-mail: lmartinez@uma.es

www.dekker.com

perature and concentration differences between the interfaces results in a vapor pressure difference between them. Evaporation takes place at the feed membrane interface. After vapor flows through the membrane pores, condensation takes place at the interface of the colder side. The vapor pressure difference is the driving force for transport, and the following relationship for the mass flux, J, may be written

$$J = C(p_{m1} - p_{m2}) \tag{1}$$

where C is the membrane distillation coefficient, whose form depends on the model used to describe the transport mechanism (1–3). In Eq. (1), p_{m1} and p_{m2} are the vapor pressures at the warm and cold membrane surfaces, respectively.

However, polarization phenomena are inevitable in MD, as has been stated by many authors (1–6). In this way the temperature and concentration (and therefore the vapor pressure) of the bulk solutions are different from those of the membrane surface. As a result, the real flux given in Eq. (1) is lower than the one that would be produced in the case if no polarization existed:

$$J^* = C(p_{b1} - p_{b2}) \tag{2}$$

We can consider the polarization effect as a loss in the driving force for transport with regard to the externally imposed force. We have measured this loss by introducing the vapor pressure polarization coefficient

$$f = \frac{p_{m1} - p_{m2}}{p_{b1} - p_{b2}} \tag{3}$$

The considerations about f will be different if the feed is water or a concentrated salt solution.

In fact, there is an extensive bibliography about MD [a summary can be found in the review of Lawson and Lloyd (3)] that approaches the calculation of the temperature polarization coefficient, τ, defined as

$$\tau = \frac{T_{m1} - T_{m2}}{T_{b1} - T_{b2}} \tag{4}$$

given the consequences that temperature polarization has in flux reduction with respect to the expected value if such a phenomenon as temperature polarization did not exist. When the feed is water [and $(T_{b1} - T_{b2})$ is less than 10°C], τ gives approximately the measurement of the reduction of the driving force imposed, since it coincides approximately with f. This is so because the exponential Antoine relation giving the vapor pressure as a function of the temperature can be linearized, and the following approximate relation can be considered (2):

$$\frac{p_{m1} - p_{m2}}{T_{m1} - T_{m2}} = \frac{p_{b1} - p_{b2}}{T_{b1} - T_{b2}} \tag{5}$$

When the feed is a concentrated solution, concentration polarization as well as temperature polarization is also inevitable. However, the effect of concentration polarization in vapor pressure reduction is generally negligible in MD (1, 6). We cannot conclude from this that the τ coefficient will give us a correct measurement of the driving force reduction because the approximation in Eq. (5) is not correct, especially if the concentration is high [although ($T_{b1} - T_{b2}$) is less than 10°C].

In this work we show that if the distillation of more and more concentrated solutions is considered, τ and f will be more and more different, and it is necessary to evaluate f if a measurement of reduction of the driving force imposed is sought. The τ coefficient does not measure the reduction of the driving force. τ and f show different tendencies with increasing feed concentrations.

The coefficients τ and f have been calculated using a transport model proposed by Schofield et al. (7). This model has been used to check the experimental flux results. Different solution concentrations, recirculation flow rates, and temperatures have been analyzed.

EXPERIMENTAL

Experimental tests were performed using a flat PTFE membrane manufactured by Gelman Instrument Co. as TF450 (80% void fraction, 60 μm thickness, 0.45 μm nominal pore size).

The experimental setup used has been described elsewere (4). The central part of the experimental device was a modified Minitan-S cell supplied by Millipore. The flat membrane was sandwiched between two equal acrylic manifolds. Silicone separators were placed between the membrane and the manifolds, creating nine feed channels and nine permeate channels, each 55 mm long, 7 mm wide, and 0.45 mm high. The effective membrane area for the transport was 34 cm^2. In all experimental runs the membrane was maintained in a horizontal position. The feed solution was pretreated in a thermostatic bath and then pumped onto the membrane low surface. Water was likewise preheated (at a lower temperature than the feed solution) in another thermostatic bath and then pumped onto the upper membrane surface. The recirculation of the fluids on both sides of the membrane was in countercurrent directions.

The temperatures of the bulk liquid phases were measured at the hot entrance ($T_{b1\text{-in}}$), the cold entrance ($T_{b2\text{-in}}$), the hot exit ($T_{b1\text{-out}}$), and the cold exit ($T_{b2\text{-out}}$) of the membrane cell. In the following study the average values

$$T_{b1} = \frac{T_{b1\text{-in}} + T_{b1\text{-out}}}{2}, \qquad T_{b2} = \frac{T_{b2\text{-in}} + T_{b2\text{-out}}}{2}$$

will be considered as the bulk temperatures of the distilland feed and the distillate permeate, respectively. These temperatures are different from the average temperatures at the hot and cold membrane sides, T_{m1} and T_{m2}, due to temperature polarization.

Different experiments were carried out for fixed temperatures in the membrane module. The feed temperature T_{b1} varied from 24 to 42°C at increments of about 5°C, and the cooling water temperature T_{b2} varied from 14 to 32°C, also at increments of about 5°C. For all these experiments, values of $(T_{b1\text{-in}} - T_{b1\text{-out}})$ and $(T_{b2\text{-out}} - T_{b2\text{-in}})$ lower than 1.5°C were obtained. The temperature difference $(T_{b1} - T_{b2})$ was 10°C in all experiments.

In the present work experiments were conducted where the feed was 0, 1, 2, 3, or 4 M sodium chloride solutions. In all cases, pure water was recirculated in the cold semicell from the beginning of the run. In all cases the recirculation flow rates on both membrane surfaces were the same. Different experiments were carried out by applying recirculation rates of 9, 11, 13, and 15 cm^3/s. Linear velocities of about 32, 39, 46, and 53 cm/s down the channel were estimated as corresponding to the recirculation rates imposed, so the Reynolds numbers in the experiments ranged from about 180 (for the lower recirculation rate, lower temperature, and higher concentration) to about 720 (for the higher recirculation rate, higher temperature, and lower concentration). The transmembrane pressure gradient was minimum for all experiments.

A water flux from the hot to the cold phase was always observed. In the experimental setup the permeate continuously flows out of the distillate reservoir, and the corresponding distillate flux was measured by collecting the liquid flowing out. In all experiments the final composition of the distillate liquid was measured, and a total salt rejection was always observed.

THEORY

The mass flux through the membrane is driven by a vapor pressure difference resulting from the imposed temperature and salt concentration differences. This mass flux may be expressed as indicated by Eq. (1). It is well known that the presence of air trapped within the membrane pores affects the value of the flux. This is because air acts as a stagnant film. In that condition it is usually accepted that the main resistances to vapor flux come from collisions of the molecules with the pore walls and with the trapped air molecules. In other words, the transport mechanism is a combined molecular/Knudsen diffusion type (2, 3) from the membrane side where the vapor pressure is higher to the membrane side where the vapor pressure is lower. So in Eq. (1) C may be expressed as

$$\frac{1}{C} = \left(\frac{\chi\delta}{\varepsilon}\right)\left|\frac{1}{1.064r\left(\dfrac{M}{RT}\right)^{0.5}} + \frac{\Upsilon_a}{D_{wa}\left(\dfrac{M}{RT}\right)}\right| \tag{6}$$

where ε is the membrane porosity, δ is the membrane thickness, χ is the tortuosity factor, r is the pore radius, M is the water molecular weight, R is the gas constant, T is the temperature, D_{wa} is the diffusion coefficient of water vapor in air, and Υ_{a} is the log mean of the mole fraction of air within the pore.

For the water–air pair we may write (8)

$$PD_{\mathrm{wa}}\ (\mathrm{K{\cdot}Pa{\cdot}m^2/s}) = 4.46 \times 10^{-9}\, T^{2.334} \tag{7}$$

where the temperature T is in Kelvin and P is the total pressure.

Equation (6) indicates that C will be slightly dependent of experimental conditions. Inspection of this equation shows that when the temperature and feed concentration change in the range studied, C will vary only by approximately $\pm 4\%$. That is, C can be considered approximately a constant.

Simultaneously to mass transport, heat transport occurs in MD. This heat Q consists of the heat conducted through the membrane and the latent heat accompanying vapor flux:

$$Q = (k_{\mathrm{m}}/\delta)(T_{\mathrm{m1}} - T_{\mathrm{m2}}) + J\Delta H_{\mathrm{v}} \tag{8}$$

where ΔH_{v} is the latent heat of vaporization and k_{m} is the thermal conductivity of the porous membrane that can be calculated from the gas (k_{g}) and solid (k_{s}) conductivities (4) by:

$$k_{\mathrm{m}} = \varepsilon k_{\mathrm{g}} + (1 - \varepsilon)k_{\mathrm{s}}$$

Due to temperature polarization, the temperatures T_{m1} and T_{m2} may vary markedly from the measurable bulk temperatures T_{b1} and T_{b2}. In order to calculate the temperature polarization coefficient τ, we consider the heat transfer to and from the membrane surface. Heat transfers for steady conditions are equal to the amount of heat transferred inside the membrane:

$$Q = h_1(T_{\mathrm{b1}} - T_{\mathrm{m1}}) = h_2(T_{\mathrm{m2}} - T_{\mathrm{b2}}) \tag{9}$$

where h_1 and h_2 are the film heat transfer coefficients.

From Eqs. (8) and (9) we can calculate

$$T_{\mathrm{m1}} = T_{\mathrm{b1}} - (T_{\mathrm{b1}} - T_{\mathrm{b2}})\frac{\dfrac{1}{h_1}}{\dfrac{1}{h_{\mathrm{c}} + h_{\mathrm{v}}} + \dfrac{1}{h_1} + \dfrac{1}{h_2}} \tag{10}$$

and

$$T_{\mathrm{m2}} = T_{\mathrm{b2}} + (T_{\mathrm{b1}} - T_{\mathrm{b2}})\frac{\dfrac{1}{h_2}}{\dfrac{1}{h_{\mathrm{c}} + h_{\mathrm{v}}} + \dfrac{1}{h_1} + \dfrac{1}{h_2}} \tag{11}$$

Marcel Dekker, Inc.
270 Madison Avenue, New York, New York 10016

where h_c is the conduction heat transfer coefficient,

$$h_c = k_m/\delta \tag{12}$$

h_v is the vapor heat transfer coefficient,

$$h_v = \frac{J\Delta H_v}{T_{m1} - T_{m2}} \tag{13}$$

and the feed and permeate film heat transfer coefficients can be estimated by means of the dimensionless Nusselt number, Nu,

$$h_i = \mathrm{Nu}_i k_i / d_h, \qquad i = 1, 2 \tag{14}$$

where 1 and 2 refer to feed and permeate, respectively. In Eq. (14), k is the fluid thermal conductivity and d_h is the hydraulic diameter. The h_i ($i = 1, 2$) coefficients can be estimated via an appropriate correlation, such as the Sieder and Tate equation for laminar flow (9):

$$\mathrm{Nu} = 1.86\left(\mathrm{RePr}\,\frac{d_h}{L}\right)^{0.33} \tag{15}$$

where L is the channel length, and Re and Pr are the Reynolds and Prandtl numbers:

$$\mathrm{Re} = d_h v\rho/\mu, \qquad \mathrm{Pr} = c_p\mu/k \tag{16}$$

with v, ρ, μ, and k the velocity, density, viscosity, and thermal conductivity of the liquid, respectively.

The evaluation of the coefficients h_c, h_v, h_1, and h_2 from the last equations allows us to calculate T_{m1} and T_{m2} from Eqs. (10) and (11). But, as ($T_{m1} - T_{m2}$) is in Eq. (13), an iterative solution is required. Initial values of T_{m1} and T_{m2} were assumed. Then, using the measured J, the value of h_v coefficient was calculated from Eq. (13). Then by using Eqs. (10) and (11), the temperatures T_{m1} and T_{m2} were obtained and compared with the initially assumed values. The calculation was repeated until the assumed values for T_{m1} and T_{m2} agreed with the calculated ones to a degree of relative error of 0.1%. In this way we determined T_{m1} and T_{m2} for each experiment.

When pure water is used as a feed liquid, the permeation flux is affected simply by the thermal boundary layers as a function of the stirring speed and temperatures. A reduction of the permeate flux occurs with an increase of salt concentration in the feed solution. This results because the decrease of the vapor pressure is in equilibrium with the feed. But the effect of solute in the feed also alters the fluid dynamics and influences the heat transfer (and therefore T_{m1} and T_{m2}, and so J) through density, thermal conductivity, and heat capacity. Finally, concentration polarization is formed by water (and no solute) permeation through the membrane, and so the solute concentration c_{m1} at the hot membrane surface becomes higher than that in the bulk solution, c_{b1}:

$$c_{m1} = c_{b1} \exp(J/\rho K) \tag{17}$$

where K is the solute mass transfer coefficient. In our experiments we evaluated the K coefficient using the Graetz–Lévêque equation:

$$\mathrm{Sh} = 1.86\left(\mathrm{ReSc}\,\frac{d_h}{L}\right)^{0.33} \tag{18}$$

where Sh and Sc are the Sherwood number and the Schmidt number:

$$\mathrm{Sh} = Kd_h/D, \qquad \mathrm{Sc} = \mu/\rho D \tag{19}$$

with D being the diffusion coefficient of the solute.

These last relations allow us to evaluate c_{m1} and so the concentration polarization coefficient, ζ:

$$\zeta = c_{m1}/c_{b1} \tag{20}$$

Summing up, if we proceed as indicated, we can know T_{m1}, T_{m2}, and c_{m1} for each experiment, and therefore evaluate the polarization coefficients τ, f, and ζ.

RESULTS AND DISCUSSION

As previously mentioned, experiments were carried out for different temperatures, feed concentrations, and recirculation rates. In order to measure the mass flux, the temperatures $T_{b1\text{-in}}$, $T_{b1\text{-out}}$, $T_{b2\text{-in}}$, and $T_{b2\text{-out}}$ were maintained constant (within ±0.1°C) for the same feed concentration and recirculation rates (all with oscillations lower than 2%).

The distillate flux was measured by weighing the water which overflows from the cold reservoir for about 30 minutes. Each distillate flux measurement was repeated at least three times. The maximum difference between the results obtained was $\pm 0.00003\ \mathrm{kg \cdot m^{-2} \cdot s^{-1}}$. The average value of the fluxes so measured was considered to be a measurement of the mass flux through the membrane. Figures 1 and 2 show these results for recirculation rates of 9 and 13 $\mathrm{cm^3/s}$, respectively, as a function of the imposed feed temperature when different feed salt concentrations were used. The flux results shown in Fig. 3 are representative of the general trend observed as the recirculation rate changes, that is, J increases slightly as the recirculation rate increases.

The results in Figs. 1–3 agree qualitatively with the behavior expected for mass flux in membrane distillation: flux increases with temperature and recirculation rate, and flux decreases as concentration feed increases. In addition, we have verified that there is good quantitative agreement between ex-

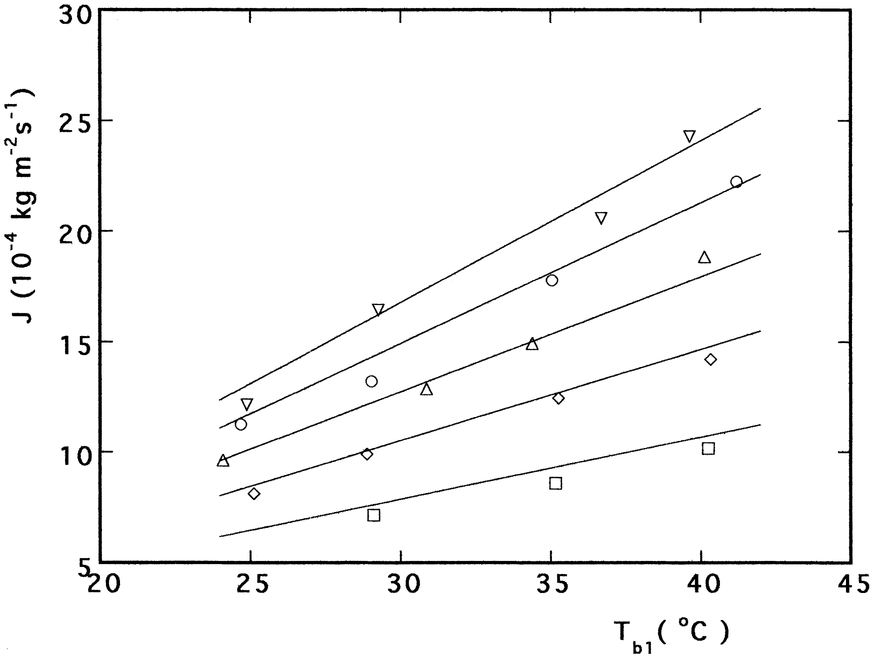

FIG. 1 Water flux vs feed temperature for a recirculation rate of 9 cm^3/s. The different symbols correspond to different hot feeds of molar concentrations: (▽) 0 M, (○) 1 M, (△) 2 M, (◊) 3 M, (□) 4 M. The solid lines correspond to model predictions for $C = 17.4 \times 10^{-7}$ kg·m^{-2}·s^{-1}·Pa^{-1}.

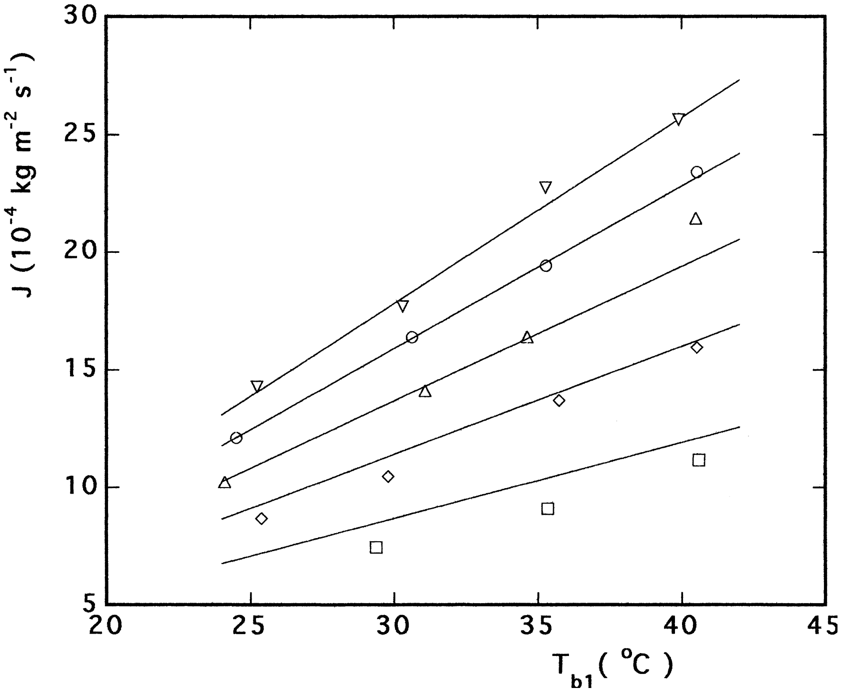

FIG. 2 Water flux vs feed temperature for a recirculation rate of 13 cm^3/s. Symbols as for Fig. 1. The solid lines correspond to model predictions for $C = 17.4 \times 10^{-7}$ kg·m^{-2}·s^{-1}Pa^{-1}.

Marcel Dekker, Inc.
270 Madison Avenue, New York, New York 10016

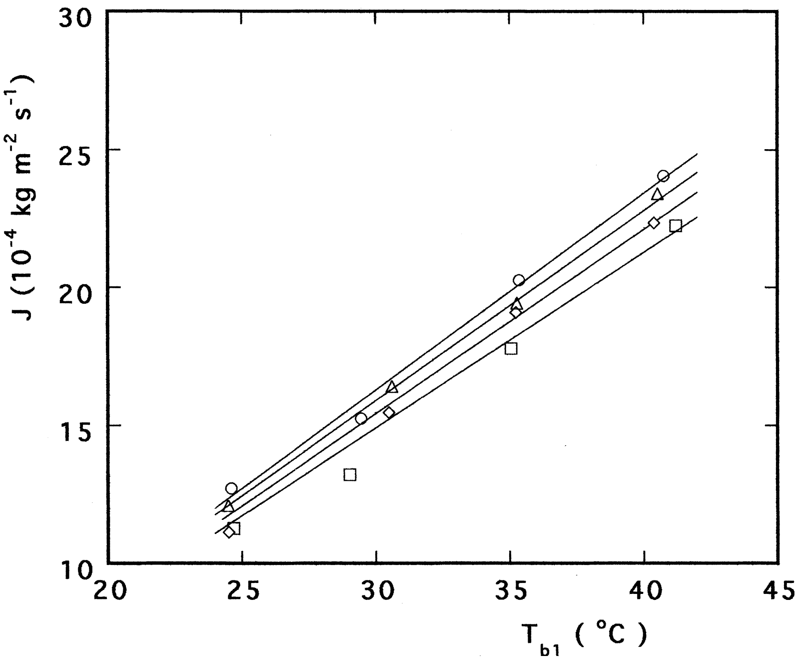

FIG. 3 Water flux vs feed temperature when feed solution was 1 M. The different symbols correspond to different recirculation rates in cm^3/s: (□) 9, (◊) 11, (△) 13, (○) 15. The solid lines correspond to model predictions for $C = 17.4 \times 10^{-7}$ kg·m^{-2}·s^{-1}·Pa^{-1}.

perimental flux results and theoretical predictions of the model described. In order to make these predictions, it is first necessary to calculate the membrane distillation coefficient C. In Eq. (6) the tortuosity factor χ is unknown, so a C value is assumed. Then the equations presented in the Theory section are used to predict the flux through the membrane for each T_{b1}, T_{b2}, and recirculation rate studied when water is the feed. The iterative method used is similar to that described for the calculation of T_{m1} and T_{m2} from the measured flux. Initial values of T_{m1} and T_{m2} are now assumed. Then, using the Antoine equation, p_{m1} and p_{m2} are calculated. Next, the predicted flux is determined by Eq. (1). By employing Eqs. (10) and (11), temperatures T_{m1} and T_{m2} are obtained and compared with the initially assumed values. The calculation is repeated until the assumed values for T_{m1} and T_{m2} agree with the calculated ones to a degree of relative error of 0.1%. Finally, the flux value predicted is obtained. Different C values are assumed, and the theoretical fluxes for the different temperatures and recirculation rates studied for water as feed are calculated. By the least-squares method, the best agreement between theoretical and experimental fluxes for water was found to be $C = 17.4 \times 10^{-7}$ kg·m^{-2}·s^{-1}·Pa^{-1}.

In Figs. 1–3 the solid lines are the theoretical predictions for this C value. Literature data on activity coefficients (10) were used when the feed was a salt solution. As can be seen, the model predictions are in good agreement with the experimental results for feed solutions other than water. There is some discrepancy between the predicted and experimental results when higher salt concentrations are used. This can be due to the reduction of flux by the occurrence of thin salt layers in some places of the membrane (11).

A value of $C = 17.4 \times 10^{-7}$ kg·m^{-2}·s^{-1}·Pa^{-1} can be obtained from Eq. (6) for a temperature of 300 K by using the manufacturer's data for porosity, thickness, and pore radius if a tortuosity factor of 1.17 is employed. A tortuosity value of 1.2 was estimated by Calabrò et al. (12) for other hydrophobic membranes used in membrane distillation.

In Figs. 4–6 the τ coefficients are shown. We have calculated these coefficients by using the iterative method described in the Theory section from the measured J values (it is not necessary to know the C value of the membrane in this calculation). From the representative results shown we can conclude the following.

- In the temperature interval studied (T_{b1} varied from 24 to 42°C), τ varies significantly, decreasing as the temperature increases. This is due to the exponential rise of the vapor pressure curve which makes the permeate flux increase substantially as the temperature rises. These larger mass

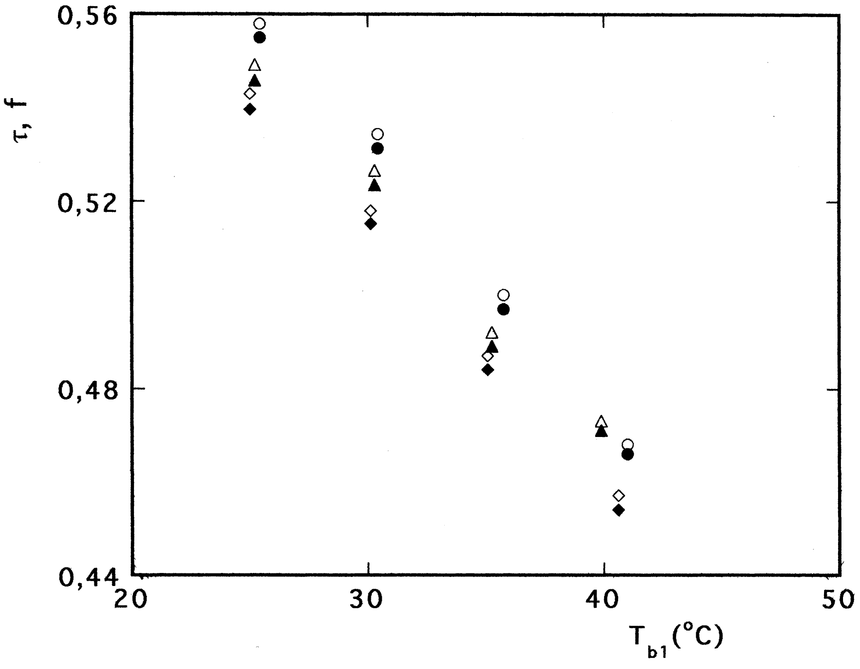

FIG. 4 Temperature polarization (open symbols) and vapor pressure polarization (solid symbols) coefficients vs feed temperature when the hot feed is water. The different symbols correspond to different recirculation rates in cm^3/s: (◊) 11, (△) 13, (○) 15.

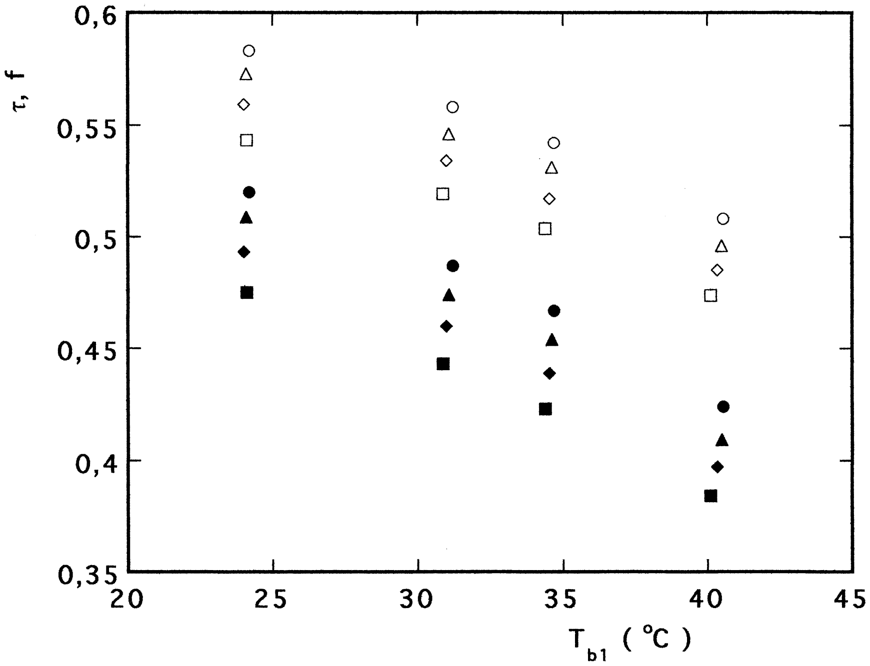

FIG. 5 Temperature polarization (open symbols) and vapor pressure polarization (solid symbols) coefficients vs feed temperature when the hot feed is a 2 M solution. Symbols as for Fig. 3.

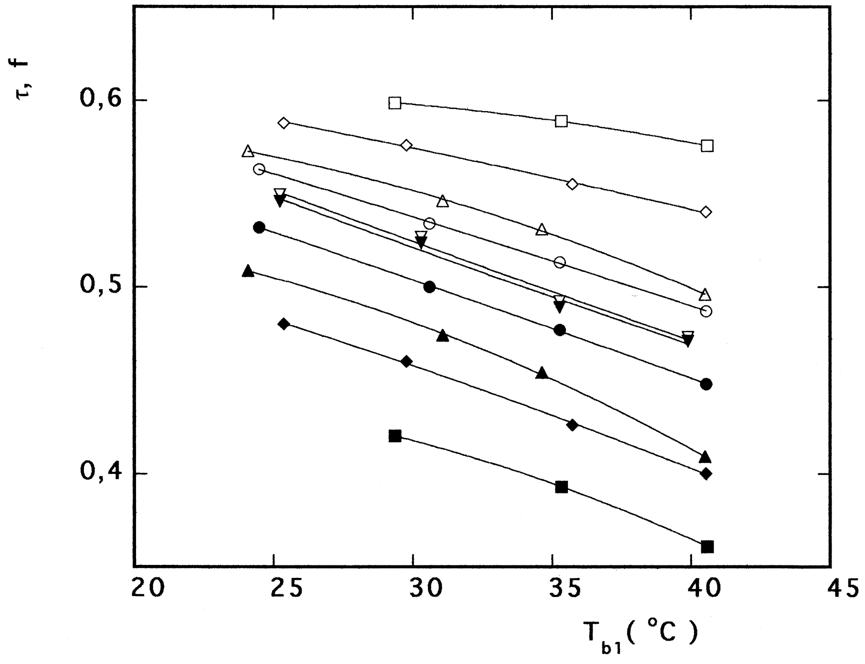

FIG. 6 Temperature polarization (open symbols) and vapor pressure polarization (solid symbols) coefficients vs feed temperature for a recirculation rate of 13 cm^3/s. Symbols as for Fig. 1. The solid lines are the fits of the results to a quadratic function.

fluxes involve more important heat fluxes through the liquid phases, increasing the temperature gradient in the boundary liquid layers and so the temperature polarization. For this reason *J* does not increase with the temperature as fast as the vapor pressure curve.

- In the recirculation rate range studied (this varies from 9 to 15 cm^3/s), the change of τ with the recirculation rate is important. The reason is that when the polarization temperature values are important, an increase of the recirculation rate enhances the heat transport, and so τ and *J* increase.
- In the concentration range studied (c_{b1} varies from 0 to 4 M), we observe an increase of τ as c_{b1} increases in correspondence with the decrease of *J* when the feed concentration increases.

As indicated previously, after evaluating τ we evaluated the concentration polarization coefficient ζ from Eqs. (17)–(20). The ζ values obtained are lower than 1.04, which shows that the effect of concentration polarization in the studied systems was small. The coefficient ζ was approximately constant with the recirculation rate as a result of two compensating contributions, the increases of *K* and *J* with the recirculation rate. As a consequence of the increase of *J* with the temperature, ζ increases as the temperature increases. Finally, ζ decreases as the feed concentration increases due to the important decrease of *J* with the feed concentration and, on a lower scale, to the increase of ρ with concentration. Figure 7 shows some representative results. We can conclude that for the mass transfer coefficients in this work (that is, for the module and the operational conditions used), membranes with higher fluxes than the membrane employed here will be necessary in order to have an important concentration polarization.

After evaluating τ (that is, T_{m1} and T_{m2}) and ζ (that is, c_{m1}), we calculated f using the bibliography data of vapor pressure (10) in order to evaluate p_{m1}, p_{m2}, p_{b1}, and p_{b2} as a function of temperature and concentration. The results obtained are shown in Figs. 4–6. From these results we can conclude:

1. The f values differ significantly from the unity value. That is, in the membrane distillation process only a part of the driving force externally imposed is effective for transport.
2. When water is used as feed, the values of τ and f are similar. In this case the value of τ can be considered to be a good measurement of the reduction of driving force imposed by the effect of polarization.
3. When c_{b1} increases, the difference between τ and f increases. This difference is important even when concentration polarization effects in vapor pressure reduction are negligible. For each concentration, f shows with the temperature and the recirculation rate the qualitative trends explained for τ.
4. When the feed is a concentrated solution, Eq. (5) is not true and the vapor

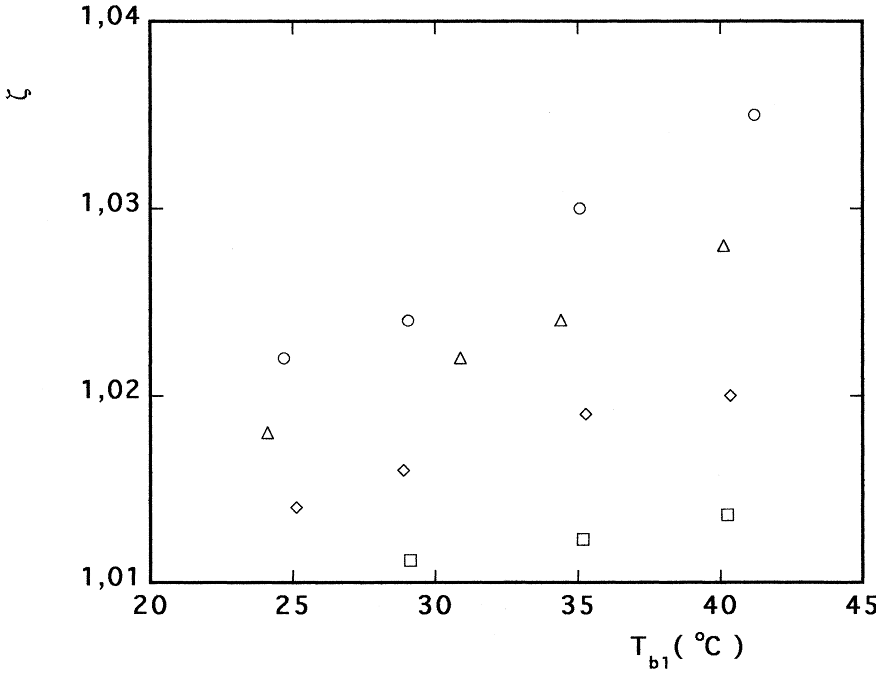

FIG. 7 Concentration polarization coefficients vs feed temperature for a recirculation rate of 9 cm^3/s. The different symbols correspond to different hot feeds of molar concentrations: (○) 1 M, (△) 2 M, (◊) 3 M, (□) 4 M.

pressure dependence with concentration must be taken into account in order to explain the f values and the important reduction in flux with regard to the one obtained with water, even when τ increases a little with the concentration. As a general conclusion, the drop of flux with rising concentrations has several causes: the temperature polarization, the decrease of the vapor pressure, and, on a lower scale, the concentration polarization. Taking into account the dependence of the vapor pressure with temperature and concentration,

$$p = p(T, c)$$

We have defined

$$J^{\mathrm{id}} = C(p^*_{\mathrm{b1}} - p^*_{\mathrm{b2}}) = C[p(T_{\mathrm{b1}}, 0) - p(T_{\mathrm{b2}}, 0)] \tag{21}$$

$$J^{\mathrm{t}} = C(p^*_{\mathrm{m1}} - p^*_{\mathrm{m2}}) = C[p(T_{\mathrm{m1}}, 0) - p(T_{\mathrm{m2}}, 0)] \tag{22}$$

$$J^{\mathrm{v}} = C[p(T_{\mathrm{m1}}, c_{\mathrm{b1}}) - p(T_{\mathrm{m2}}, 0)] \tag{23}$$

where p^*_{b1}, p^*_{b2}, p^*_{m1}, and p^*_{m2} are the vapor pressures of pure water at temperatures T_{b1}, T_{b2}, T_{m1}, and T_{m2}, respectively. The J^{id} values represent the ideal situation whose temperature and concentration polarization does not exist and where the reduction of the vapor pressure that occurs when $c \neq 0$ has not been taken into account. The differences between the J^{id} and J^{t} values represent the effect of temperature polarization, and the relation J^{t}/J^{id} coincides approximately with τ. The differences between the J^{t} and J^{v} values represent flux reduction due to the decrease of the vapor pressure of the solution with respect to pure water; these differences are a increasing function of the feed concentration. Finally, the differences between J^{v} and J values represent the effect of concentration polarization. The results obtained for J^{id}, J^{t}, and J^{v}, together with the ones obtained experimentally, J, are shown in Figs. 8 and 9 for some representative experimental conditions for 1 and 3 M feed concentrations, respectively. In both cases the effects of temperature polarization are similar, while the effect of the dependence of the vapor pressure with concentration is significantly higher for the 3 M solution. The effects of the concentration polarization are negligible, as can be seen in the drawings.

Summing up, τ is not a measurement of the total reduction of the driving force imposed for concentrated solutions. When the feed is a concentrated solution, f gives the measurement of the mentioned reduction. Likewise, the temperature boundary layers exert a large influence in mass transport. The permeate flux might be substantially higher if we had no temperature polar-

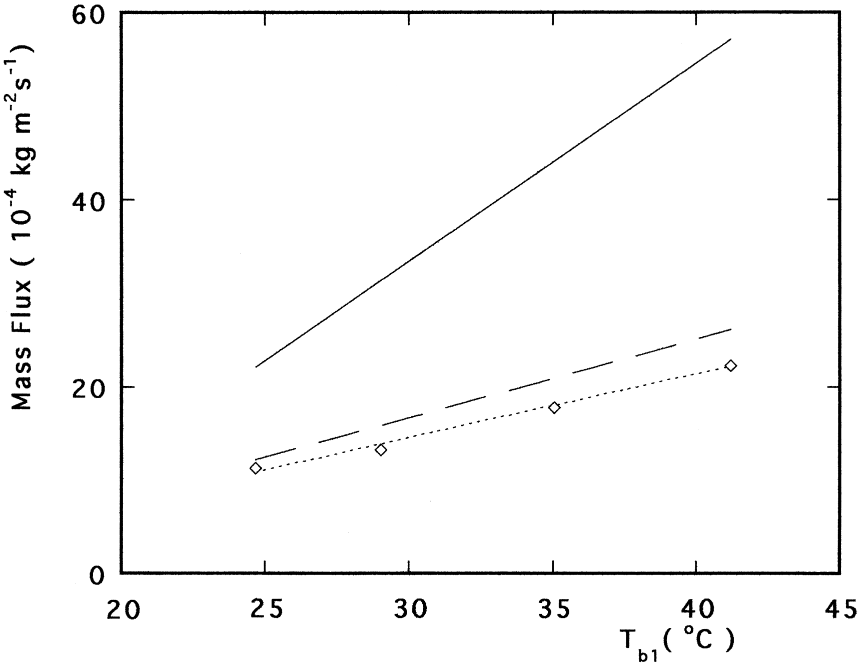

FIG. 8 Mass flux through the membrane vs feed temperature for a recirculation rate of 9 cm^3/s and a 1 M hot feed solution. The lines correspond to J^{id} (——), J^{t} (- - -) and J^{v} ($\cdots$) values calculated as defined in Eqs. (21)–(23) using a C value of 17.4×10^{-7} kg·m^{-2}s^{-1}·Pa^{-1}.

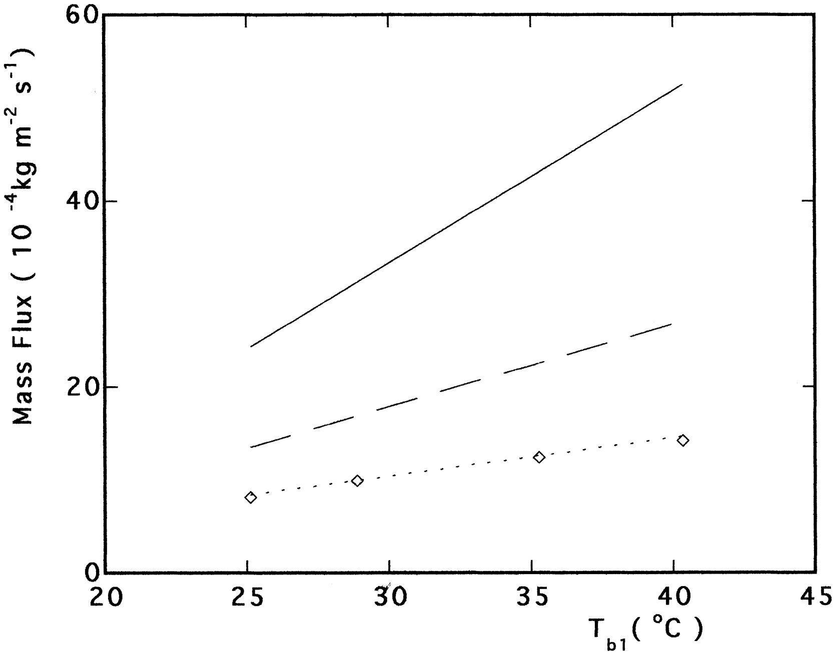

FIG. 9 Mass flux through the membrane vs feed temperature for a recirculation rate of 9 cm^3/s and a 3 M hot feed solution. Symbols as for Fig. 8.

ization. As the concentration increases, the effect of vapor pressure in the reduction of the driving force imposed becomes more important. In all cases studied, the effect of concentration polarization is small.

NOMENCLATURE

c	molar concentration ($mol \cdot L^{-1}$)
c_p	specific heat ($J \cdot kg^{-1} \cdot K^{-1}$)
C	membrane distillation coefficient ($kg \cdot m^{-2} \cdot s^{-1} \cdot Pa^{-1}$)
d_h	hydraulic diameter of channel (m)
D	diffusion coefficient of solute ($m^2 \cdot s^{-1}$)
D_{wa}	diffusion coefficient of water vapor in air ($m^2 \cdot s^{-1}$)
f	vapor pressure polarization coefficient (—)
h	heat transfer coefficient ($W \cdot m^{-2} \cdot K^{-1}$)
J	mass flux through the membrane ($kg \cdot m^{-2} \cdot s^{-1}$)
J^*	as defined in Eq. (2) ($kg \cdot m^{-2} \cdot s^{-1}$)
J^{id}	as defined in Eq. (21) ($kg \cdot m^{-2} \cdot s^{-1}$)
J^t	as defined in Eq. (22) ($kg \cdot m^{-2} \cdot s^{-1}$)
J^v	as defined in Eq. (23) ($kg \cdot m^{-2} \cdot s^{-1}$)
k	thermal conductivity of the liquid ($W \cdot m^{-1} \cdot K^{-1}$)

k_m	thermal conductivity of the membrane ($\mathrm{W \cdot m^{-1} \cdot K^{-1}}$)
k_g	thermal conductivity of the air ($\mathrm{W \cdot m^{-1} \cdot K^{-1}}$)
k_s	thermal conductivity of the solid phase of the membrane ($\mathrm{W \cdot m^{-1} \cdot K^{-1}}$)
K	solute mass transfer coefficient ($\mathrm{m \cdot s^{-1}}$)
L	channel length (m)
M	water molecular weight ($\mathrm{kg \cdot mol^{-1}}$)
Nu	Nusselt number (—)
P	total pressure (Pa)
p	pressure of water vapor (Pa)
p^*	vapor pressure of pure water at the same temperature as the solution (Pa)
Pr	Prandtl number (—)
Q	heat flux ($\mathrm{W \cdot m^{-2}}$)
R	gas constant ($\mathrm{J \cdot mol^{-1} \cdot K^{-1}}$)
r	pore radius (m)
Re	Reynolds number (—)
Sc	Schmidt number (—)
Sh	Sherwood number (—)
T	temperature (K)
v	linear velocity ($\mathrm{m \cdot s^{-1}}$)

Greek Letters

χ	tortuosity factor (—)
δ	membrane thickness (m)
ε	porosity (—)
μ	liquid viscosity ($\mathrm{Pa \cdot s}$)
ΔH_v	latent heat of vaporization ($\mathrm{J \cdot kg^{-1}}$)
ρ	liquid density ($\mathrm{kg \cdot m^{-3}}$)
τ	temperature polarization coefficient (—)
ζ	concentration polarization coefficient (—)
Υ_a	log mean of the mole fraction of air (—)

Subscripts

b	in the bulk phase
c	conduction
m	at the membrane surface
v	vapor
1	hot feed solution
2	cold water

REFERENCES

1. G. C. Sarti, C. Gostoli and S. Matulli, "Low Energy Cost Desalination Process Using Hydrophobic Membranes," *Desalination, 56*, 277–286 (1985).
2. R. W. Schofield, A. G. Fane, and C. J. D. Fell, "Heat and Mass Transfer in Membrane Distillation," *J. Membr. Sci., 33*, 299–313 (1987).
3. K. W. Lawson and D. R. Lloyd, "Review. Membrane Distillation," *Ibid., 124*, 1–25 (1997).
4. L. Martínez-Díez and M. I. Vázquez-González, "Temperature Polarization in Mass Transport through Hydrophobic Porous Membranes," *AIChE J., 42*(7), 1844–1852 (1996).
5. A. Velázquez and J. I. Mengual, "Temperature Polarization Coefficients in Membrane Distillation," *Ind. Eng. Chem. Res., 34*, 583–590 (1995).
6. V. Calabro, *Transport Phenomena Involved in Membrane Distillation Processes*, Workshop on Membrane Distillation, Osmotic Distillation and Membrane Contactors, Cetraro, Italy, 1998.
7. R. W. Schofield, A. G. Fane, C. J. D. Fell, and R. Macoun, "Factors Affecting Flux in Membrane Distillation," *Desalination, 77*, 279–294 (1990).
8. R. B. Bird, W. E. Stewart, and E. N. Lightfoot, *Transport Phenomena*, Wiley, New York, NY, 1967.
9. J. P. Holman, *Heat Transfer*, McGraw-Hill, New York, NY, 1989.
10. R. A. Robinson and R. H. Stokes, *Electrolyte Solutions*, Butterworths, London, 1959.
11. K. Schneider, W. Kölz, R. Wollbeck, and S. Ripperger, "Membranes and Modules for Transmembrane Distillation," *J. Membr. Sci., 39*, 25–42 (1988).
12. V. Calabrò, B. L. Jiao, and E. Drioli, "Theoretical and Experimental Study on Membrane Distillation in the Concentration of Orange Juice," *Ind. Eng. Chem. Res., 33*, 1803–1808 (1994).

Received by editor August 30, 1999
Revision received December 1999

Downloaded At: 10:57 25 January 2011

Request Permission or Order Reprints Instantly!

Interested in copying and sharing this article? In most cases, U.S. Copyright Law requires that you get permission from the article's rightsholder before using copyrighted content.

All information and materials found in this article, including but not limited to text, trademarks, patents, logos, graphics and images (the "Materials"), are the copyrighted works and other forms of intellectual property of Marcel Dekker, Inc., or its licensors. All rights not expressly granted are reserved.

Get permission to lawfully reproduce and distribute the Materials or order reprints quickly and painlessly. Simply click on the "Request Permission/Reprints Here" link below and follow the instructions. Visit the U.S. Copyright Office for information on Fair Use limitations of U.S. copyright law. Please refer to The Association of American Publishers' (AAP) website for guidelines on Fair Use in the Classroom.

The Materials are for your personal use only and cannot be reformatted, reposted, resold or distributed by electronic means or otherwise without permission from Marcel Dekker, Inc. Marcel Dekker, Inc. grants you the limited right to display the Materials only on your personal computer or personal wireless device, and to copy and download single copies of such Materials provided that any copyright, trademark or other notice appearing on such Materials is also retained by, displayed, copied or downloaded as part of the Materials and is not removed or obscured, and provided you do not edit, modify, alter or enhance the Materials. Please refer to our Website User Agreement for more details.

Order now!

Reprints of this article can also be ordered at
http://www.dekker.com/servlet/product/DOI/101081SS100100237